

## Static quark free energies at finite temperature with two flavors of improved Wilson quarks

---

**Y. Maezawa , S. Ejiri, T. Hatsuda, N. Ishii, N. Ukita**

*Department of Physics, The University of Tokyo,*

*Bunkyo-ku, Tokyo 113-0033, Japan*

*E-mail: maezawa@nt.phys.s.u-tokyo.ac.jp*

**S. Aoki and K. Kanaya**

*Graduate School of Pure and Applied Sciences, University of Tsukuba,*

*Tsukuba, Ibaraki 305-8571, Japan*

Polyakov loop correlations at finite temperature in two-flavor QCD are studied in lattice simulations with the RG-improved gluon action and the clover-improved Wilson quark action. From the simulations on a  $16^3 \times 4$  lattice, we extract the free energies, the effective running coupling  $g_{\text{eff}}(T)$  and the Debye screening mass  $m_D(T)$  for various color channels of heavy quark-quark and quark-anti-quark pairs above the critical temperature. The free energies are well approximated by the screened Coulomb form with the appropriate Casimir factors. The magnitude and the temperature dependence of the Debye mass are compared to those of the next-to-leading order thermal perturbation theory and to a phenomenological formula given in terms of  $g_{\text{eff}}(T)$ . Also we made a comparison between our results with the Wilson quark and those with the staggered quark previously reported.

*XXIVth International Symposium on Lattice Field Theory*

*July 23-28, 2006*

*Tucson, Arizona, USA*

---

Speaker.

## 1. Introduction

The interaction between heavy quarks in a hot QCD medium is one of the most important quantities to characterize the properties of the quark-gluon plasma (QGP). Experimentally, it is related to the fate of the charmoniums and bottomoniums in the QGP created in relativistic heavy ion collisions. In this report, we present our recent studies on the heavy-quark free energy in dynamical simulations of two-flavor QCD with the Wilson fermion. We study the free energy of a quark ( $Q$ ) and an antiquark ( $\bar{Q}$ ) separated by the spatial distance  $r$  in the color singlet and octet channels, and also study the free energy of  $Q$  and  $Q$  in the color anti-triplet and sextet channels. We adopt the Coulomb gauge fixing for the gauge-non-singlet free energies. By fitting the numerical results with the screened Coulomb form, we extract an effective running coupling and the Debye screening mass in each channel as a function of temperature.

We find that (i) the free energies in the different channels at high temperature ( $T > 2T_c$ ) can be well described by the channel-dependent Casimir factor together with the channel-independent running coupling  $g_{\text{eff}}(T)$  and the Debye mass  $m_D(T)$ , (ii) the next-to-leading order result of the Debye mass in thermal perturbation gives better agreement with  $m_D(T)$  on the lattice than that of the leading order, (iii)  $g_{\text{eff}}(T)$  and  $m_D(T)$  may be related through the leading order formula,  $m_D(T) = \frac{1}{1 + N_f/6} g_{\text{eff}}(T)T$ , so that most of the higher order and non-perturbative effects on the Debye mass may be absorbed in  $g_{\text{eff}}(T)$  for  $T > 1.5T_c$ , and (iv) there is a quantitative discrepancy of  $m_D(T)$  between our results using the Wilson quark and those using the staggered quark even at  $T = 4T_c$ .

## 2. Lattice action and simulation parameters

We employ the renormalization group improved gluon action and clover improved Wilson quark action with two-flavors. The line of constant physics, on which the quark mass (or the ratio of pseudo-scalar and vector meson masses) is kept fixed in the space of the coupling  $\beta$  and the hopping parameter  $K$ , has been studied in refs. [1] using the same action and is discussed further in ref. [2]. We perform the simulations on the lines of constant physics for the quark masses corresponding to  $m_\pi = m_\rho = 0.65$  and 0.80. Ten (seven) different temperatures are taken in the interval  $T = 1.00T_c - 4.02T_c$  for  $m_\pi = m_\rho = 0.65$  ( $T = 1.07T_c - 3.01T_c$  for  $m_\pi = m_\rho = 0.80$ ) on a  $N_s \times N_t = 16^3 \times 4$  lattice. The hybrid Monte Carlo algorithm is employed to generate full QCD configurations, and the free energy in each color channel is measured using 500 configurations at every ten trajectories after thermalization of 400-1000 trajectories. The statistical errors are determined by a jackknife method with the bin-size of 10 configurations.

## 3. Heavy quark free energies

The free energy of static quarks on a lattice may be described by the correlations of the Polyakov loop:  $\Omega(\mathbf{x}) = \prod_{\tau=1}^{N_t} U_4(\tau; \mathbf{x})$  where  $N_t$  is a lattice size in the temporal direction, and the  $U_\mu(\tau; \mathbf{x}) \in SU(3)$  is the link variable. By appropriate gauge fixing (such as the Coulomb gauge fixing), one can define the free energy in various color channels separately [3]: the color singlet  $Q\bar{Q}$

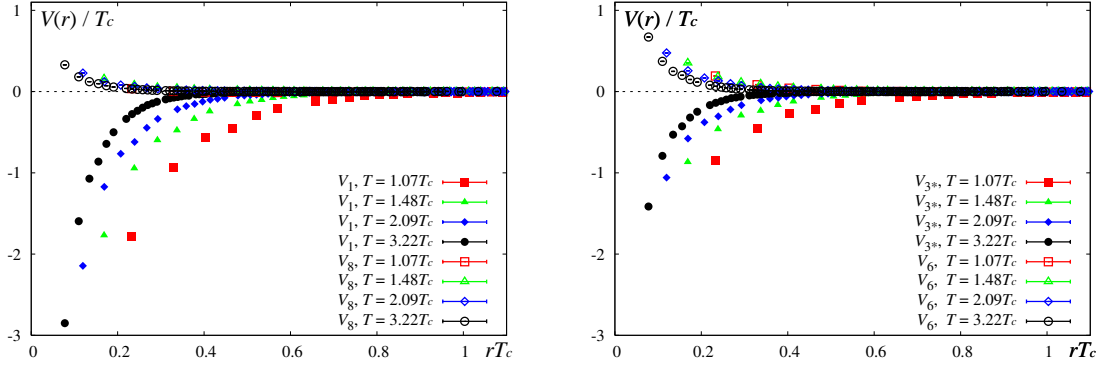


**Figure 1:** Simulation results of the normalized free energies scaled by  $T_c$  for color singlet and octet  $Q\bar{Q}$  channels (left) and color anti-triplet and sextet  $QQ$  channels (right) at  $m_\pi=m_\rho = 0.65$  and several temperatures.

channel **(1)**, the color octet  $Q\bar{Q}$  channel **(8)**, the color anti-triplet  $QQ$  channel **(3)**, and the color sextet  $QQ$  channel **(6)** :

$$e^{F_{\mathbf{1}}(r;T)=T} = \frac{1}{3} \text{hTr} \Omega^\dagger(\mathbf{x}) \Omega(\mathbf{y}) i; \quad (3.1)$$

$$e^{F_{\mathbf{8}}(r;T)=T} = \frac{1}{8} \text{hTr} \Omega^\dagger(\mathbf{x}) \text{Tr} \Omega(\mathbf{y}) i - \frac{1}{24} \text{hTr} \Omega^\dagger(\mathbf{x}) \Omega(\mathbf{y}) i; \quad (3.2)$$

$$e^{F_{\mathbf{6}}(r;T)=T} = \frac{1}{12} \text{hTr} \Omega(\mathbf{x}) \text{Tr} \Omega(\mathbf{y}) i + \frac{1}{12} \text{hTr} \Omega(\mathbf{x}) \Omega(\mathbf{y}) i; \quad (3.3)$$

$$e^{F_{\mathbf{3}}(r;T)=T} = \frac{1}{6} \text{hTr} \Omega(\mathbf{x}) \text{Tr} \Omega(\mathbf{y}) i - \frac{1}{6} \text{hTr} \Omega(\mathbf{x}) \Omega(\mathbf{y}) i; \quad (3.4)$$

where  $r = |\mathbf{x} - \mathbf{y}|$

We introduce normalized free energies ( $V_{\mathbf{1}}; V_{\mathbf{8}}; V_{\mathbf{6}}; V_{\mathbf{3}}$ ) which are expected to approach zero at large distances above  $T_c$ . This is equivalent to defining the free energies by dividing the right-hand sides of Eq. (3.1) – (3.4) by  $\text{hTr} \Omega^2$ .

The normalized free energies are shown in Fig. 1 for color singlet and octet  $Q\bar{Q}$  channels (left) and color anti-triplet and sextet  $QQ$  channels (right) for  $m_\pi=m_\rho = 0.65$  and  $T = T_c$ . They are “attractive” in the color singlet and anti-triplet channels and “repulsive” in the color octet and sextet channels. Also they become weak at long distances as  $T$  increases due to the effect of Debye screening. These behaviors are qualitatively similar to the case in the quenched simulations with the Lorenz gauge reported in ref. [4].

To study the screening effects in each color channel more closely, we fit the free energies by the screened Coulomb form:

$$V_M(r;T) = C(M) \frac{\alpha_{\text{eff}}(T)}{r} e^{-m_D(T)r}; \quad (3.5)$$

where  $\alpha_{\text{eff}}(T)$  and  $m_D(T)$  are the effective running coupling and Debye screening mass, respectively. The  $C(M) = \frac{1}{2} \sum_{a=1}^8 t_1^a \frac{q_{i_M}}{2}$  is the Casimir factor for each color channel ( $M$ ) defined as

$$C(\mathbf{1}) = \frac{4}{3}; \quad C(\mathbf{3}) = \frac{2}{3}; \quad C(\mathbf{8}) = \frac{1}{6}; \quad C(\mathbf{6}) = \frac{1}{3}; \quad (3.6)$$

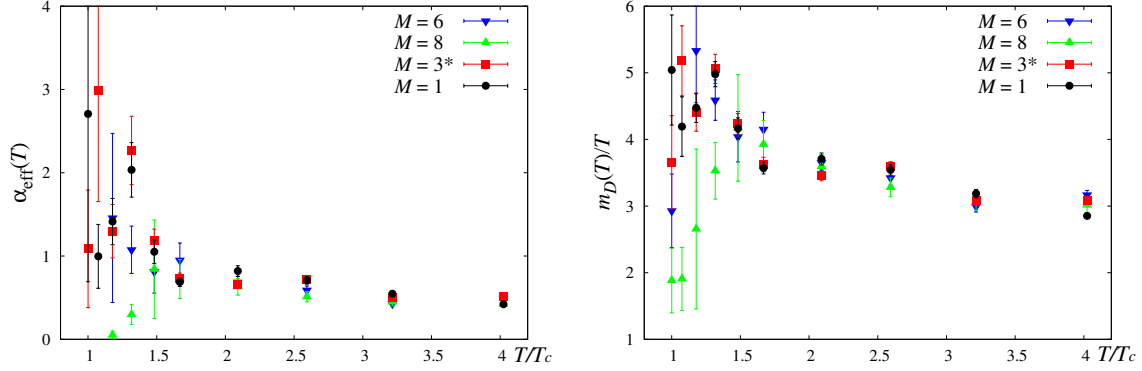


**Figure 2:** The effective running coupling  $\alpha_{\text{eff}}(T)$  (left) and Debye screening mass  $m_D(T)$  (right) for each color channel as a function of temperature from the large distance behavior of the potentials at  $m_\pi=m_\rho = 0.65$ .

Here, it is worth stressing that, with the improved actions we adopt, the rotational symmetry is well restored in the heavy quark free energies [5]. Therefore we do not need to introduce terms correcting lattice artifacts at short distances in eq. (3.5) to fit the data shown in Fig.1.

The Debye screening effect is defined through the long distance behavior of  $V_M(r;T)$ . In order to determine the appropriate fit range, we estimate the effective Debye mass from a ratio of normalized free energies:

$$m_D(T; r) = \frac{1}{\Delta r} \log \frac{V_M(r)}{V_M(r + \Delta r)} = \frac{1}{\Delta r} \log \left( 1 + \frac{\Delta r}{r} \right) ; \quad (3.7)$$

Investigating the plateau of  $m_D(T; r)$ , we choose the fit range to be  $\frac{r}{T} = 1.5$ . Systematic errors due to the difference of the fit range are about 10% for  $T > 2T_c$ .

The results of the  $\alpha_{\text{eff}}(T)$  and  $m_D(T)$  are shown in Fig. 2 for  $m_\pi=m_\rho = 0.65$ . Similar behavior in both results are obtained for  $m_\pi=m_\rho = 0.80$ . We find that there is no significant channel dependence of  $\alpha_{\text{eff}}(T)$  and  $m_D(T)$  at sufficiently high temperature ( $T > 2T_c$ ). In other words, the channel dependence of the free energy at high temperature may be well absorbed in the kinematical Casimir factor as first indicated in a quenched study [4].

#### 4. Debye mass on the lattice and that in perturbative theory

Let us first compare the Debye mass on the lattice with that calculated in thermal perturbation theory. First of all, the 2-loop running coupling is given by

$$g_{2l}^2(\mu) = \beta_0 \ln \frac{\mu}{\Lambda_{\overline{MS}}} + \frac{\beta_1}{\beta_0} \ln \ln \frac{\mu}{\Lambda_{\overline{MS}}} ; \quad (4.1)$$

where the argument in the logarithms may be written as  $\mu = \Lambda_{\overline{MS}} = (\mu=T) (T=T_c) (T_c = \Lambda_{\overline{MS}})$  where we adopt  $T_c = \Lambda_{\overline{MS}}^{n_f=2} = 0.656$  for the last factor [1, 6]. The renormalization point  $\mu$  is assume to be in a range  $\mu = \pi T \sim 3\pi T$ . By using  $g_{2l}$  as a function of  $T=T_c$ , the Debye screening mass in the

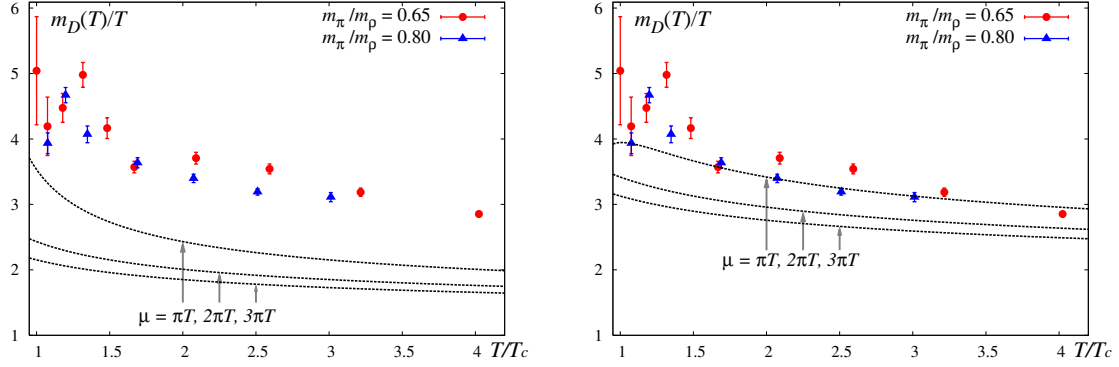


**Figure 3:** The Debye screening masses  $m_D(T)$  at  $m_\pi=m_\rho = 0.65$  and  $0.80$  in the color singlet channel together with that calculated in the leading-order (left) and next-to-leading-order (right) thermal perturbation theory shown by the dashed lines.  $\mu$  is the renormalization point chosen at  $\mu = \pi T; 2\pi T; 3\pi T$ .

leading-order (LO) thermal perturbation is given as  $m_D^{\text{LO}}(T) = T \sqrt{1 + N_f g_{2l}^2(T)}$ , where the effect of the quark mass is neglected.

Figure 3(left) shows the  $m_D(T)$  in the color singlet channel compared with  $m_D^{\text{LO}}(T) = T \sqrt{1 + N_f g_{2l}^2(T)}$  for  $\mu = \pi T; 2\pi T$  and  $3\pi T$ . We find that the screening mass  $m_D^{\text{LO}}(T)$  in the leading order perturbation theory does not reproduce the lattice data, which has been known in the quenched QCD [7] and in the full QCD with the staggered quark [8].

To study higher-order contributions in the thermal perturbation theory, we consider the Debye mass in the next-to-leading-order calculated by the hard thermal resummation given in ref. [9].

$$\frac{m_D^{\text{NLO}}}{T} = \sqrt{1 + \frac{N_f}{6} g_{2l}^2(T)} \sqrt{1 + g_{2l}^2(T) \frac{3}{2\pi} \frac{1}{1 + N_f g_{2l}^2(T)} \ln \frac{2m_D^{\text{LO}}}{m_{\text{mag}}}} \frac{1}{2} + o(g^2) : \quad (4.2)$$

Here  $m_{\text{mag}}$  denotes the magnetic screening mass assumed to be of the form  $m_{\text{mag}}(T) = C_m g^2(T) T$ . Since the factor  $C_m$  cannot be determined in the perturbation theory due to the infrared problem, we adopt  $C_m \approx 0.482$  calculated in quenched lattice simulations [7] as a typical value. (If we fit  $C_m$  from our lattice data  $m_D(T = 4.02T_c)$  with  $\mu = 2\pi T$ , we obtain  $C_m \approx 0.40$ ).  $m_D^{\text{NLO}}(T)$  for different choice of the renormalization point is shown in Fig. 3(right) by the dashed lines together with the lattice data. They have approximately 50% enhancement from the leading order results and lead to a better agreement with the lattice data.

## 5. Phenomenological relation between $\alpha_{\text{eff}}$ and $m_D$

So far, we have fitted the free energies on the lattice with  $\alpha_{\text{eff}}$  and  $m_D$  as independent parameters. Here let us introduce an ‘‘effective’’ running coupling as  $g_{\text{eff}}(T) = \sqrt{4\pi\alpha_{\text{eff}}(T)}$ . Suppose that  $m_D(T)$  is expressed by  $g_{\text{eff}}(T)$  according to the leading-order perturbation,

$$\frac{m_D(T)}{T} = \sqrt{1 + \frac{N_f}{6} g_{\text{eff}}^2(T)} : \quad (5.1)$$

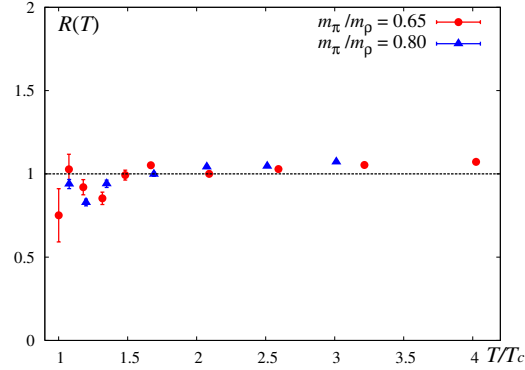


**Figure 4:** The ratio  $R(T)$  in the text which is supposed to be close to unity if  $m_D(T) = \sqrt{\frac{q}{1 + N_f=6 g_{\text{eff}}(T)T}}$  holds. The data are for the color singlet channel.

This relation means that the following ratio  $R$  evaluated from our lattice data should be close to unity, i.e.  $R(T) = \frac{m_D(T)}{(1 + N_f=6) \sqrt{\frac{q}{4\pi\alpha_{\text{eff}}(T)}}} \approx 1$ .

In Fig. 4, the lattice data of  $R(T)$  for the singlet channel are shown as a function of  $T$ . We find that  $R(T)$  is consistent with unity even at  $T > 1.5T_c$  with 10% accuracy. This is a non-trivial observation particularly near  $T_c$  and suggests that the major part of the higher-order effects and non-perturbative effects of  $m_D(T)$  can be expressed by the effective running coupling  $g_{\text{eff}}(T)$ . We note that a similar effective coupling defined through the lattice potential was discussed to improve the lattice perturbation theory at  $T = 0$  [10].

## 6. Comparison with the staggered quark

Finally, we compare the results of  $\alpha_{\text{eff}}(T)$  and  $m_D(T)$  obtained with the Wilson quark action (present work) with those with an improved staggered quark action. The latter simulation was done on a  $16^3 \times 4$  and with a quark mass corresponding to  $m_\pi = m_\rho = 0.70$  [8]. The comparison is shown in Fig. 5 for  $\alpha_{\text{eff}}(T)$  (left panel) and  $m_D(T)$  (right panel). Although  $\alpha_{\text{eff}}(T)$  does not show significant difference between the two actions,  $m_D(T)$  in the Wilson action is systematically higher than that of the staggered action by about 20% even at  $4T_c$ . This difference should be further investigated by increasing the temporal lattice size.

## 7. Summary

We have studied the free energy of  $QQ$  and  $Q\bar{Q}$  systems in 2-flavor QCD at finite temperature using the lattice simulation with the renormalization group improved gluon action and the clover improved Wilson quark action on a  $16^3 \times 4$  lattice. The free energy normalized to be zero at large separation show attraction (repulsion) in the color singlet and anti-triplet channels (color octet and sextet channels).

The screened Coulomb form with the Casimir factor and with the effective coupling  $\alpha_{\text{eff}}(T)$  and the Debye screening mass  $m_D(T)$  as free parameters is used to fit the free energy in each channel.  $\alpha_{\text{eff}}(T)$  and  $m_D(T)$  become universal and all the channel dependence is absorbed in the

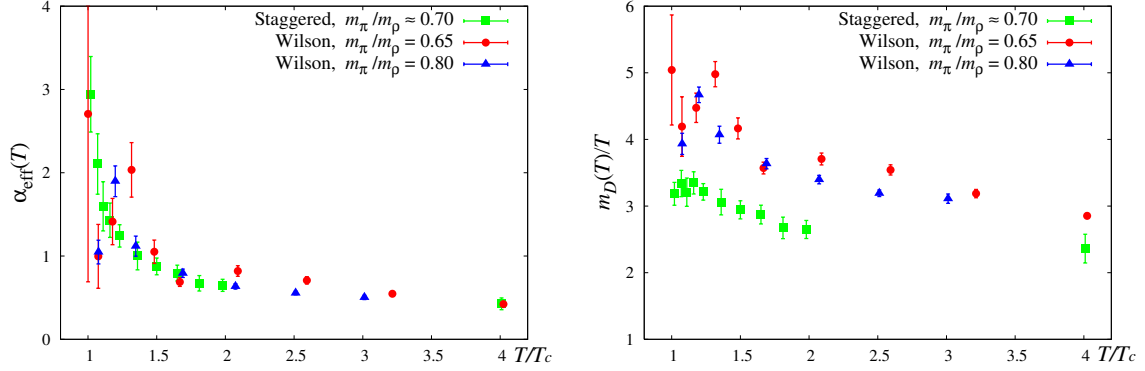


**Figure 5:** Comparison of the  $\alpha_{\text{eff}}(T)$ (left) and  $m_D(T)$ (right) between the results of the Wilson quark action and staggered quark action.

Casimir factor for  $T > 2T_c$ . The magnitude and the  $T$ -dependence of the Debye mass  $m_D(T)$  is consistent with the next-to-leading order calculation in the perturbation theory as well as the leading order perturbation with the “effective” running coupling.

The results from an improved Wilson quark action are compared with these from an improved staggered quark action with the same lattice size and similar quark mass. The  $\alpha_{\text{eff}}(T)$  does not show appreciable difference between the two actions, whereas the  $m_D(T)$  of the Wilson quark action is systematically higher than that of the staggered quark action by 20%. The simulations with larger lattice sizes especially in the temporal direction (such as  $N_t = 6$  and larger) should be carried out as well as those at small quark masses.

**Acknowledgements:** We thank O. Kaczmarek for providing us the data from a staggered quark action. This work is in part supported by Grants-in-Aid of the Japanese Ministry of Education, Culture, Sports, Science and Technology, (Nos. 13135204, 15540251, 17340066, 18540253, 18740134). SE is supported by the Sumitomo Foundation (No. 050408), and YM is supported by JSPS. This work is in part supported also by the Large-Scale Numerical Simulation Projects of ACCC, Univ. of Tsukuba.

## References

- [1] A. Ali Khan *et al.* (CP-PACS Collaboration), *Phys. Rev.* **D63** (2001) 034502; **64** (2001) 074510.
- [2] N. Ukita, S. Ejiri, T. Hatsuda, N. Ishii, Y. Maezawa, S. Aoki and K. Kanaya, in proceedings of *Lattice 2006*. PoS (LAT2006) 150.
- [3] S. Nadkarni, *Phys. Rev.* **D33** (1986) 3738; **34** (1986) 3904.
- [4] A. Nakamura and T. Saito, *Prog. Theor. Phys.* **111** (2004) 733; **112** (2004) 183.
- [5] S. Aoki *et al.* (CP-PACS Collaboration), *Phys. Rev.* **D60** (1999) 114508.
- [6] M. Gockeler *et al.*, *Phys. Rev.* **D73** (2006) 014513.
- [7] A. Nakamura, T. Saito and S. Sakai, *Phys. Rev.* **D69** (2004) 014506.
- [8] O. Kaczmarek and F. Zantow, *Phys. Rev.* **D71** (2005) 114510.

- [9] A. K. Rebhan, *Phys. Rev. D***48** (1993) 3967.
- [10] G. P. Lepage and P. B. Mackenzie, *Phys. Rev. D***48** (1993) 2250.